

Seismic protection of the benchmark highway bridge with passive hybrid control system

Arijit Saha^{*1}, Purnachandra Saha¹ and Sanjaya Kumar Patro²

¹School of Civil Engineering, KIIT University, Odisha, India

²Department of Civil Engineering, Veer Surendra Sai University of Technology, Odisha, India

(Received March 20, 2017, Revised April 30, 2018, Accepted May 22, 2018)

Abstract. The present paper deals with the optimum performance of the passive hybrid control system for the benchmark highway bridge under the six earthquakes ground motion. The investigation is carried out on a simplified finite element model of the 91/5 highway overcrossing located in Southern California. A viscous fluid damper (known as VFD) or non-linear fluid viscous spring damper has been used as a passive supplement device associated with polynomial friction pendulum isolator (known as PFPI) to form a passive hybrid control system. A parametric study is considered to find out the optimum parameters of the PFPI system for the optimal response of the bridge. The effect of the velocity exponent of the VFD and non-linear FV spring damper on the response of the bridge is carried out by considering different values of velocity exponent. Further, the influences of damping coefficient and vibration period of the dampers are also examined on the response of the bridge. To study the effectiveness of the passive hybrid system on the response of the isolated bridge, it is compared with the corresponding PFPI isolated bridges. The investigation showed that passive supplement damper such as VFD or non-linear FV spring damper associated with PFPI system is significantly reducing the seismic response of the benchmark highway bridge. Further, it is also observed that non-linear FV spring damper hybrid system is a more promising strategy in reducing the response of the bridge compared to the VFD associated hybrid system.

Keywords: benchmark highway bridge; polynomial friction pendulum isolator; fluid viscous damper; non-linear FV spring damper; hybrid control; SIMULINK; evaluation criteria

1. Introduction

Highway bridge structure plays a very important role in the surface transportation network in everyday life under the category of communication and economic demand. The catastrophic failure of the bridge seriously hampers relief and economic demand. In the past few earthquakes, stability of the bridge has been affected by the seismic events. Due to the simple connection between the deck and pier, bridges are extensively vulnerable when it is subjected to a strong seismic event. Conventional deck and pier rigid connection of the bridge limit the deck horizontal displacement but increase the base shear and superstructural acceleration which is more vulnerable. It has been observed that the failure of the bridge is initiated by piers and propagated to the deck, as a result of expansion of joint failure or shear key failure or excessive displacement of the deck, leading to the collapse of the bridge. For maximum earthquake ground motion, the fundamental period of the bridge is near about the predominant period of the ground motion. The fundamental period of the bridge structure is in the range of 0.3 to 1 sec. The seismic force can be reduced if the fundamental period of the structure is lengthened or the energy dissipation capabilities of the structure are increased.

Seismic isolation technique is an alternative and innovative design approach to decouple the structure and ground from the destructive impact of the earthquake ground motion and, dissipate the input energy of the structure which was introduced into it.

Over the past few years, an impressive effort has been made in the development and improvisation of the base isolation in the different bridges. To develop an economically earthquake protective structure, it requires striking a balance between strength stiffness and energy dissipation. The main objective of the earthquake protective structure is to dissipate the input energy through inelastic deformation. It is not cost-effective to keep the structure in elastic region during severe seismic events. Several seismologists have proposed that base isolated structures are vulnerable against a large period, pulse type ground motion near the fault zones (Hall *et al.* 1995, Heaton *et al.* 1995). Near field, earthquakes are distinguished with one or more intense velocity pulse in the velocity time history response. These long period pulses are clearly going to have a huge effect on the isolation system with large isolator displacement. To suit extensively large isolator displacement, there is a requirement of a very large seismic gap and size of the isolator has to be increased. Other than these pre-requisites, the requirement for flexible utility associations includes additional expense. Besides, if satisfactory seismic gaps or expansion joints are not provided, it may lead to undesirable pounding effect.

Park *et al.* (2003) present the hybrid control system for

*Corresponding author, Ph.D. Student
E-mail: arijitsaha081@gmail.com

protection of cable-stayed bridge, consisting of LRB and hydraulic actuators or magnetorheological fluid dampers. This hybrid control system is more superior compared to the passive control system and marginally better than the active and semi-active control system. (Jangid 2004) studied the seismic response of bridges isolated by LRB under bi-directional excitation and proposed that restoring force interaction of the LRB has a significant effect on the seismic response of the bridges. The effectiveness of the hybrid control strategy consists of the passive viscous damper and semi-active dampers as investigated by (He and Agrawal 2007). The authors found that hybrid control system is quite effective in reducing seismic response and also protecting the passive damper from strong earthquake ground motion. (Soneji and Jangid 2007) examined the influence of hybrid control system for the protection of cable-stayed bridge under real earthquake ground motion. Viscous fluid damper is used as a passive supplement damping device, associated with elastomeric and sliding isolation system. The author has shown that hybrid control system is effective in reducing the seismic response of the cable-stayed bridge. (Matsagar and Jangid 2008) evaluated the response of historical buildings, bridges and liquid storage tanks subjected to base isolation in the retrofitting works. However, authors showed that seismic response reduces significantly in the retrofitting structure compared to the conventional structure. (Abdel Raheem and Hayashikawa 2013) observed that passive energy dissipation device can improve the seismic response of the cable-stayed bridge tower, which also includes the tower drift, moment and axial load. (Takewaki *et al.* 2013) examined the performance of the viscous and elastic-plastic hysteretic type damper in the base isolated building and reported that elastic plastic hysteretic damper is not much effective compared to the viscous type damper through the bounded aspect ratio. (Chen *et al.* 2014) found that hybrid control system (MR damper and isolator) is quite effective in controlling the seismic responses of the structure. (Xie and Sun 2014) evaluated that passive hybrid system with viscous fluid damper can improve the failure mode of the cable-stayed bridge in a transverse direction.

Geng *et al.* (2014) studied the influence of passive control device for the multi-tower cable-stayed bridge with the partially longitudinal constraint system, and found that viscous fluid dampers are more promising in improving the seismic response. (Mishra *et al.* 2015) carried out the seismic response of the bridge installed with Shape-memory-alloy-based rubber bearing (SMABRB) under the random excitation. This effectively reduced the isolator displacement with a marginal increase in deck acceleration. The effectiveness of the passive non-linear FV spring damper also has been demonstrated on the benchmark highway bridge by Saha *et al.* (2015). Xing *et al.* (2015) examined the performance of the viscous fluid damper, friction pendulum sliding bearing and transverse yielding metallic damper on the transverse response reduction of the pier of the cable-stayed bridge and showed that viscous fluid dampers are very effective in reducing the response. (Markou *et al.* 2016) investigated the seismic performance of the residential building with bi-linear and tri-linear

assisted linear viscous damper hybrid isolation system. (Kataria and Jangid 2016) studied the performance of the semi-active variable stiffness damper for the horizontally curved bridges. It was found that SAVSD is effective in seismic response mitigation of curved bridges. Amiri *et al.* (2017) investigated the pounding effect of a single-story building isolated by triple friction pendulum bearing.

Several researchers have proposed that it may be possible to reduce the large bearing displacement under the near-fault ground motion with the help of passive devices for additional energy dissipation (Soneji and Jangid 2007, Dicleli 2007). Thereby, it will be interesting to study the effectiveness of the passive hybrid control system consisting of fluid viscous damper or non-linear fluid viscous spring damper, used as a passive supplement device and polynomial friction pendulum isolator (PFPI) as an isolation device on the seismic response of the benchmark highway bridge. In the present study passive hybrid control system for earthquake protection of highway bridges under different ground motion is investigated. The specific objectives of the present study are; (i) To investigate the performance of the different passive hybrid systems subjected to different types of ground motion, (ii) To study the effect of device parameters on different responses of the bridge, (iii) To find out an optimum parameter of the all control systems that provide an optimal response control of the bridge.

2. Description of the benchmark highway bridge

A Finite element model of the 91/5 highway overcrossing located in the Orange Country of Southern California has been developed by Agrawal *et al.* (2005, 2009). The seismic assessment criteria of the bridge emphatically considered due to the location of the bridge are within 20 km of the fault line, the Whittier-Elsinore fault and the Newport-Inglewood fault. The distance of the Whittier fault is 11.6 km to the north-east and Newport-Inglewood fault is 20 km to the south-west of the bridge. The bridge consists of a cast-in-place pre-stressed concrete box girder with continuous two spans of 58.5 m four-lane highway. The two abutments of the bridge have 33° skewed abutments. The bridge consists of three cell deck on the top of 6.9 m height. The deck is restrained by 31.4 m long pre-stressed outrigger, which is resting on two groups of piles; each pile group consists of 49 concrete friction piles. In the numerical simulation model, four Lead rubber bearing (LRB) is provided at each abutment whereas in the actual bridge, traditional nonseismic elastomeric pads are provided in the place of LRB with four passive fluid dampers. The finite element model is developed in ABAQUS, which has a total of 108 nodes, 70 beam elements, 24 springs, 24 dashpots and 8 user-defined elements. In ABAQUS B31 beam element is considered to model the deck and bent and rigid link is considered for abutment and deck-ends. The total mass of the superstructure is considered with all non-structural elements, but the contribution of their stiffness properties to the bridge is neglected. The damping of the superstructure is considered to have the function of both

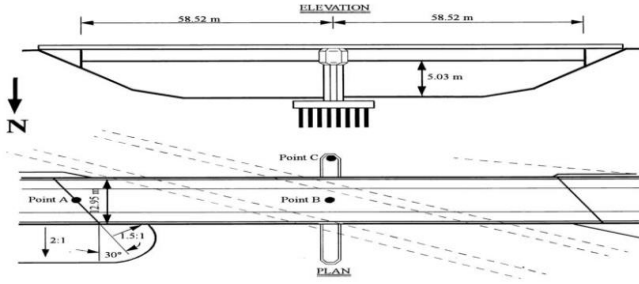


Fig. 1 Elevation and Plan of the benchmark highway bridge (Agrawal *et al.* 2005, 2009)

Table 1 Definition of the evaluation criteria considered for this study by (Agrawal *et al.* 2005, 2009)

Peak response	Norm response
Peak base shear (J_1)	Norm base shear (J_9)
$J_1 = \max \left\{ \frac{\max_{i,t} F_{bi}(t) }{F_{Ob}^{\max}} \right\}$	$J_9 = \max \left\{ \frac{\max_{i,t} \ F_{bi}(t)\ }{\ F_{Ob}^{\max}\ } \right\}$
Peak base moment (J_2)	Norm base moment (J_{10})
$J_2 = \max \left\{ \frac{\max_{i,t} M_{bi}(t) }{M_{Ob}^{\max}} \right\}$	$J_{10} = \max \left\{ \frac{\max_{i,t} \ M_{bi}(t)\ }{\ M_{Ob}^{\max}\ } \right\}$
Peak mid-span displacement (J_3)	Norm base moment (J_{11})
$J_3 = \max \left\{ \max_{i,t} \left \frac{y_{mi}(t)}{y_{Om}^{\max}} \right \right\}$	$J_{11} = \max \left\{ \max_i \left \frac{y_{mi}(t)}{y_{Om}^{\max}} \right \right\}$
Peak mid-span acceleration (J_4)	Norm mid-span acceleration (J_{12})
$J_4 = \max \left\{ \max_{i,t} \left \frac{\ddot{y}_{mi}(t)}{\ddot{y}_{Om}^{\max}} \right \right\}$	$J_{12} = \max \left\{ \max_i \left \frac{\ddot{y}_{mi}(t)}{\ddot{y}_{Om}^{\max}} \right \right\}$
Peak abutment displacement (J_5)	Norm abutment displacement (J_{13})
$J_5 = \max \left\{ \max_{i,t} \left \frac{y_{bi}(t)}{y_{Ob}^{\max}} \right \right\}$	$J_{13} = \max \left\{ \max_i \left \frac{y_{bi}(t)}{y_{Ob}^{\max}} \right \right\}$
Peak ductility (J_6)	Norm ductility (J_{14})
$J_6 = \max \left\{ \max_{j,t} \left \frac{\phi_j(t)}{\phi^{\max}} \right \right\}$	$J_{14} = \max \left\{ \max_{j,t} \left \frac{\phi_j(t)}{\phi^{\max}} \right \right\}$

mass and stiffness. The Raleigh damping parameters are considered, 5% modal damping ratio in first and second modes. Two center columns are modeled as a bilinear hysteresis model. The moment-curvature behavior of the column is considered as a bilinear and considered as two components: linear and elasto-plastic components. Plan and elevation of the benchmark highway bridge are shown in Fig. 1. From 3D finite element model of the bridge developed in ABAQUS, the first six frequencies of vibration are obtained as follows. The first mode is torsional with a natural time period of $T_1=0.813$ sec. The second mode is torsional coupled with vertical with a natural time period of $T_2=0.781$ sec. The third and fourth modes are vertical and transverse with natural time period $T_3=0.645$ sec and $T_4=0.592$ sec, respectively. The fifth and sixth modes are second vertical and second transverse with natural time period $T_5=0.565$ sec and 0.307 sec, respectively.

To evaluate the performance of the passive hybrid system, a set of 21 evaluation criteria's (J_1 - J_{21}) have been developed. The evaluation criteria J_1 - J_8 indicates reduction of the peak response quantities of the bench mark highway bridge. J_9 - J_{14} measures the norm response of the benchmark bridge. J_{15} - J_{21} is related to the control system. When passive isolation system is used, the criterion J_{17} (Peak control power) and J_{18} (Total control power) are zero, J_{20} (Number of sensor) and J_{21} are used to evaluate the seismic response of the benchmark bridge. Table 1 shows the detailed definition of the evaluation criteria considered for this study.

3. Seismic isolation and passive damper

3.1 Polynomial Friction Pendulum Isolator (PFPI).

In order to improve the performance of the sliding isolation system through sliding isolator with variable curvature, PFPI system is introduced by (Lu *et al.* 2013). The isolator has a sliding surface with variable curvature choosing the fifth order polynomial geometric function $y(x)$. More importantly, the stiffness and frequency of the isolator is the continuous function of the isolator displacement. The system consists of an articulated slider which is moving on a surface based on the polynomial function.

The horizontal shear force of the PFPI isolator is for $y'(x) \ll 1$

$$\begin{Bmatrix} F_{xb} \\ F_{yb} \end{Bmatrix} = \begin{pmatrix} W & 0 \\ 0 & W \end{pmatrix} \begin{Bmatrix} y'(x_b) \\ y'(y_b) \end{Bmatrix} + \begin{Bmatrix} f_x \\ f_y \end{Bmatrix} \quad (1)$$

x_b and y_b are the bearing displacement in two orthogonal horizontal directions; f_x and f_y are the frictional force in two orthogonal horizontal directions. Where W is the vertical load and μ is the coefficient of friction and $y'(x)$ is the second order derivative of the polynomial equation. Secant Stiffness of PFPI isolator is

$$k_r(x) = \frac{u_r(x)}{x} = \frac{Wy'(x)}{x} \quad \text{for } x = x_b, y_b \quad (2)$$

The instantaneous isolation period $T(x)$

$$T(x) = 2\pi \sqrt{\frac{x}{gy'(x)}} \quad \text{for } x = x_b, y_b \quad (3)$$

Fifth order polynomial equation can be chosen for defining the isolation surface of PFPI

$$y(x) = (1/6)ax^6 + (1/4)cx^4 + (1/2)ex^2 \quad \text{for } x = x_b, y_b \quad (4)$$

$$y'(x) = \frac{u_r(x)}{W} = ax^5 + cx^3 + ex \quad \text{for } x = x_b, y_b \quad (5)$$

The mechanical property of PFPI depends on the three polynomial coefficients a , c and e .

\bar{K}_1 and \bar{K}_2 be the isolator secant stiffness at two different isolator displacement D_1 and D_2 .

\bar{K}_0 is the normalized initial stiffness at $x = 0$, i.e., $y''(0) = \bar{K}_0$

\bar{K}_1 is the isolator secant stiffness at $x= D_1$, i.e., $y''(D_1) = \bar{K}_1$

\bar{K}_2 is the isolator secant stiffness at $x= D_2$, i.e., $y''(D_2) = \bar{K}_2$

It has been shown in this section that the mechanical property of the PFPI system is designed by endorsing the three coefficients a , c and e of the six order polynomial equation of the isolation surface defined by Eq. (6). For the design convenience of the PFPI isolation system, the three polynomial coefficients a , c and e are purely mathematical. It will be initially changed over into different parameters (T_0, T_1, T_2, D_1, D_2) that have more engineering meaning. In this way five, parameters are considered for the design of the PFPI system. The feasible value ranges, of the parameters, are achieved in such a way so that it satisfies the multiple objective performances of the PFPI system.

Where T_0, T_1, T_2 are the initial, first and second period; D_1 and D_2 are the first and second displacement of the PFPI. A solution of this simultaneous equation leads to convert the polynomial coefficients a, c, e into the five engineering parameters $\bar{K}_0, \bar{K}_1, \bar{K}_2, D_1, D_2$ which are more meaningful than the original coefficients.

$$a = \frac{-\left(\frac{D_2}{D_1}\right)^2 (\bar{K}_1 - \bar{K}_0) + (\bar{K}_2 - \bar{K}_0)}{D_1^2 D_2^2 \left[\left(\frac{D_2}{D_1}\right)^2 - 1 \right]},$$

$$c = \frac{\left(\frac{D_2}{D_1}\right)^4 (\bar{K}_1 - \bar{K}_0) - (\bar{K}_2 - \bar{K}_0)}{D_2^2 \left[\left(\frac{D_2}{D_1}\right)^2 - 1 \right]}, e = \bar{K}_0 \quad (6)$$

The stiffness of the isolator can be defined as

$$\bar{k}_j = \frac{4\pi^2}{T_j^2 g} \quad \text{for } j = 0, 1, 2 \quad (7)$$

3.1.2 Hysteretic model for frictional forces

In this study characteristic of the force-deformation behavior of the PFPI system is modeled using the theory proposed by Wen (1976). For this model, frictional force mobilized in the sliding system can be modeled as

$$f_x = F_s Z_x \quad (8)$$

$$f_y = F_s Z_y \quad (9)$$

$$F_s = \mu mg \quad (10)$$

Where F_s is the limiting value of the frictional force in which sliding system can be subjected. Where μ, m , and g are the coefficients of friction of the sliding system, the mass of the bridge deck and acceleration due to gravity, respectively. The hysteretic displacement components Z_x and Z_y satisfy the following non-linear first order differential equation expressed as

$$q\dot{Z}_x = \alpha\dot{x}_b - \beta|\dot{x}_b|Z_x|Z_x|^{n-1} - \tau\dot{x}_b Z_x^n \quad (11)$$

$$q\dot{Z}_y = \alpha\dot{y}_b - \beta|\dot{y}_b|Z_y|Z_y|^{n-1} - \tau\dot{y}_b Z_y^n \quad (12)$$

Where q is the yield displacement of the frictional force loop, Dimensionless parameters α, β, τ and n are controlling the shape of the hysteresis loop. Parameter n is the integer constant which controls the smoothness of transition elastic to plastic state. Reducing the unknown parameter with a very much characterized physical property, by applying $\left(\frac{\alpha}{\beta+\gamma}\right)=1$ constraint. The parameters considered for this present study are: $q=0.1$ cm, $\alpha=1, \beta=\tau=0.5$. The hysteretic displacement component Z_x and Z_y are bounded by ± 1 for sliding and non-sliding phases of the isolator.

3.2 Viscous Fluid Damper (VFD)

VFD dissipates energy by passing the fluid through the orifice; therefore VFD is extensively used in mitigating the seismic response of the bridge. VFD not only reduces the structural displacement, but it dissipates the energy through the whole system.

$$F_d(t) = c \operatorname{sgn}(\dot{u}(t)) |\dot{u}(t)|^\alpha \quad (13)$$

Where F_d is the damping force, C is the damping coefficient, $\dot{u}(t)$ is the relative velocity between two ends of the damper, $\operatorname{sgn}(\cdot)$ is the Signum function and α is called velocity exponent. Fluid viscous dampers with velocity exponent (α), between 0.5 and 2, have been extensively used in earthquake engineering studies. Velocity exponent equal to indicates linear VFD, whereas velocity exponent $0 < \alpha < 1$ indicates non-linear VFD. Non-linear VFD with $\alpha < 1$ minimizes the damper force at high velocity shock, in order to limit overloading in the damper and connected systems. In this study, the effect of linear and non-linear VFD with PFPI on the seismic response of the benchmark highway bridge is examined

3.3 Non-linear FV spring damper.

Non-linear FV spring damper comprises of silicon-based liquid filled empty chamber and one cylinder. The fundamental concept of the non-linear FV spring damper depends on a compressible silicon liquid passing through the annular space, between the piston head and internal

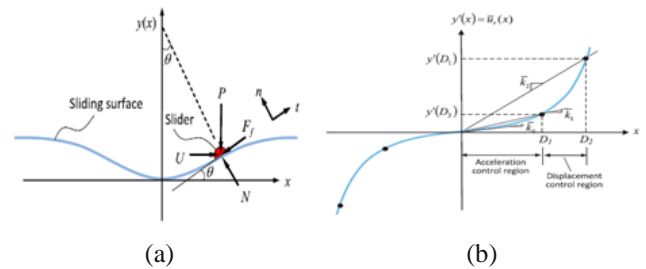


Fig. 2 (a) Force component on the slider of PFPI (b) Normalized restoring stiffness (Lu et al. 2013)

Table 2 Details of the ground motion record used in this study

Earthquake	Type	Magnitude	PGA(g) EW	PGA(g) NS	Peak velocity EW (m/s)	Peak velocity NS (m/s)
North Palm Springs (1986)	Far field	M6.0	0.492	0.612	0.733	0.338
Chi-Chi (1999)	Near fault	M7.6	1.157	0.417	1.147	0.456
Elcentro (1940)	Far field	M7.0	0.313	0.215	0.298	0.302
Rinadi (1994)	Near fault	M6.7	0.838	0.472	1.661	0.730
Turkbolu (1999)	Near fault	M7.1	0.728	0.822	0.564	0.621
Kobe (1995)	Near fault	M6.9	0.509	0.503	0.373	0.366

casing, which is pressurized by a static pre-load imposed in the manufacturing phase. The characterization of the re-centering capacity of the device depends on the initial pressurization of the silicon fluid. The total reaction force developed by the non-linear FV spring damper is the summation of the damping force ($F_d(t)$) and elastic force ($F_e(t)$) of the spring, corresponding to their damping and spring function, (Sorace and Terenzi 2001). Damping force ($F_d(t)$) and elastic force ($F_e(t)$) can be expressed as

$$F_d(t) = c \operatorname{sgn}(\dot{u}(t)) |\dot{u}(t)|^\alpha \quad (14)$$

Where F_d is the damping force, C is the damping coefficient, $\dot{u}(t)$ is the relative velocity between two ends of the damper, $\operatorname{sgn}(\cdot)$ is the signum function and α is called velocity exponent.

$$F_e(t) = k_2 u(t) + \frac{(k_1 - k_2) u(t)}{\left[1 + \left| \frac{k_1 u(t)}{F_0} \right|^R \right]^{1/R}} \quad (15)$$

Where $F_e(t)$ is the elastic force of spring, K_1 and K_2 are the translation stiffness of the response branches situated below and beyond the preload threshold, $u(t)$ is the relative displacement, F_0 is the manufacturing imposed preload, R is the integer exponent.

$$F_0 = \frac{F_{\max}}{n} \quad (16)$$

$$k_2 = \frac{4\pi^2 m}{T^2} \quad (17)$$

$$k_1 = 15k_2 \quad (18)$$

where F_{\max} is the maximum reaction force under quasi-static loading maximum reaction force developed by the device, T is the vibration period of the spring and n is the explicit design variable in the range of 2 to 7 (Sorace and Terenzi 2001).

4. Numerical study

To verify the effectiveness of the proposed passive

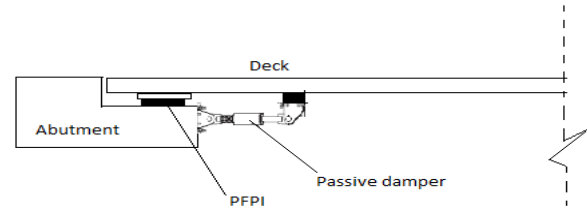


Fig. 3 Position of PFPI system and damper in the bridge

hybrid control strategy, a set of simulation is performed for the six historical earthquakes specified in the highway benchmark bridge problem (Agrawal *et al.* 2005, 2009). The six ground motions are, namely (i) North Palm Spring (1986) (ii) TUC084 component of Chi-Chi earthquake, Taiwan (1999) (iii) Elcentro component of Imperial Valley earthquake (iv) Rinadi component of Northridge (1984) (v) Bolu component of Duzce, Turkey (1999) earthquake and (vi) Nishi-Akashi component of Kobe (1995) earthquake. The peak ground acceleration and peak ground velocity of the selected earthquake ground motions are shown in Table 2. These ground motions are assumed to act simultaneously with all support along the transverse and longitudinal directions of the bridge. In this numerical study, the vertical components of the ground motions are neglected, and there is no biaxial interaction between the x and y component of the frictional force. For moderate to high fundamental period structure, the effect of vertical ground motion does not include an error in the calculation (Shakib and Fuladgar 2003, Nakata *et al.* 2004). Passive isolation device and dampers are considered, connecting the bridge deck and abutments. The control arrangement considered in this study consists of sixteen PFPI devices and sixteen dampers which can act in both the longitudinal and transverse directions, in eight different positions. The devices connect the deck with abutments and are located under the deck. Eight PFPI and eight dampers are acting on the bridge in the longitudinal direction and, the remaining are acting in the transverse direction.

To evaluate the performance of the passive hybrid system, the response quantities selected are the peak base shear in pier, peak base moment, peak mid-span acceleration, peak mid-span displacement and peak ductility responses of the bridge, respectively. The relative displacement of the bridge abutment is crucial from the design point of view of the isolation system and expansion joint. The effects of different isolator parameters are analyzed, that are subjected to different peak responses of the bridge. These parameters include (1) first displacement of PFPI (D_1) and (2) first and second time periods of the PFPI. A parametric study is performed to investigate the effect of variation of the damping coefficient of the VFD (considering linear, i.e., $\alpha=1$ and non-linear, i.e., α between 0.4-2) and the effect of variation of the vibration period of the FV spring damper on the peak responses of the bridge. The results of the parametric study are presented in Figs. 4, 5 and 6. The performance of the PFPI is characterized by the initial period (T_0), first period (T_1), second period (T_2), first displacement (D_1), second displacement (D_2) and coefficient of friction (μ).

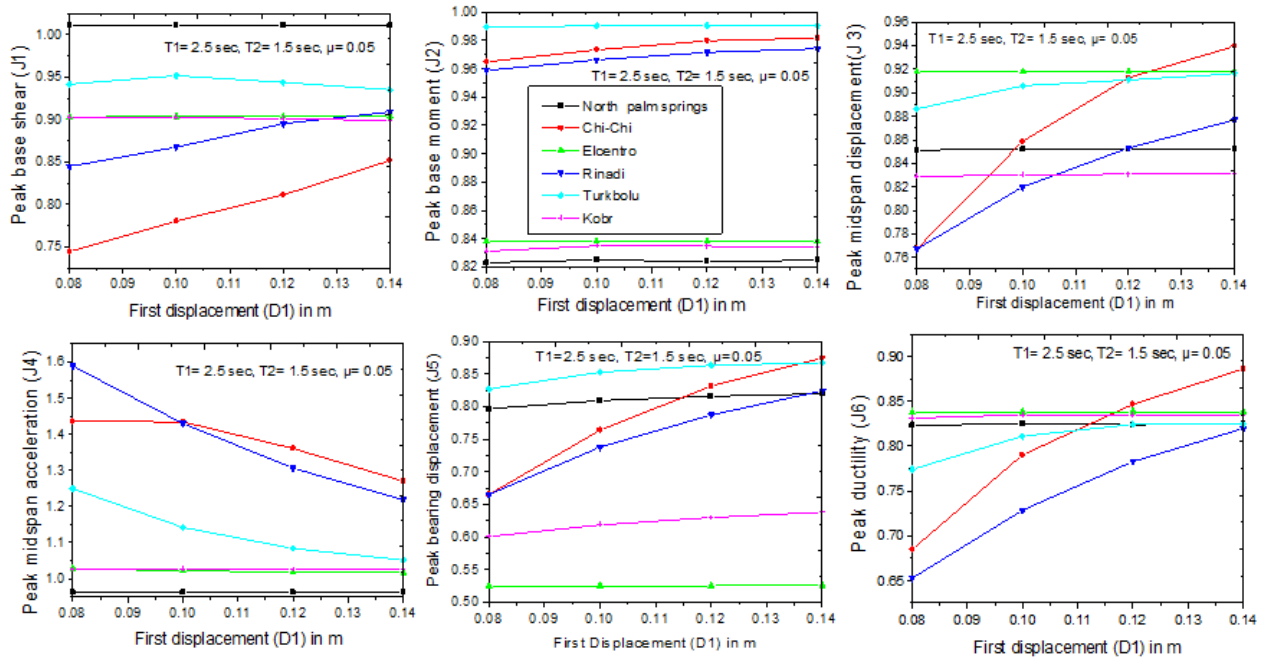


Fig. 4 Effect of first displacement (D_1) of PFPI on peak base shear, peak base moment, peak mid-span displacement, peak mid-span acceleration, peak bearing displacement and peak ductility

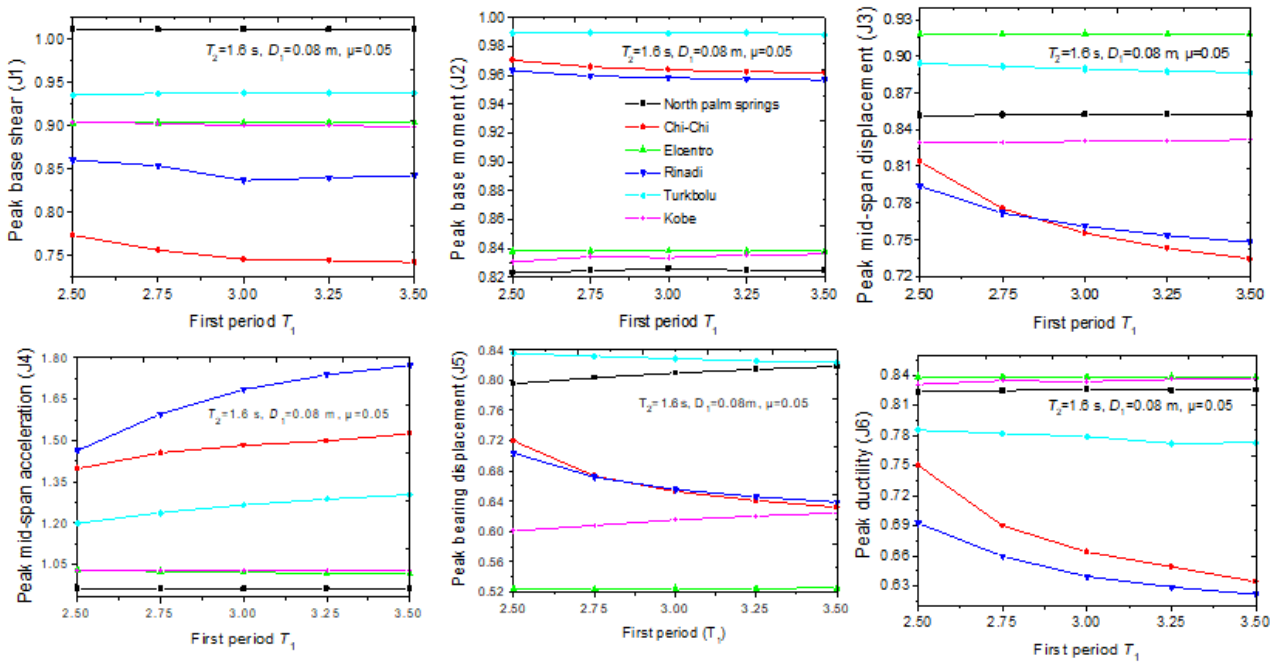


Fig. 5 Effect of First period of PFPIs (T_1) on peak base shear, peak base moment, peak mid-span displacement, peak mid-span acceleration, peak bearing displacement and peak ductility

Except for coefficient of friction, the other four parameters are varied in order to know their impacts on the seismic response of the benchmark highway bridge and to find out their optimal parameters. In Fig. 4 the first displacement (D_1) of PFPI is varied from 0.08 m to 0.14 m, keeping the other isolator parameters (D_2/D_1)=1.5 ref, first period (T_1)=2.5 s, second period (T_2)=1.5 sec and coefficient of friction (μ)=0.05. It can be seen from the Fig 4 that, with an increase in the first displacement of PFPI, the peak responses increase significantly (except peak mid-

span acceleration) for Chi-Chi and Rinadi earthquakes, which is not desirable. Therefore the first displacement, which is 0.08 m, can be considered as an optimum value. Further, it can be seen from Fig. 5 that, after the first period of 3 sec, with a further increase in the first period, the peak base shear response does not decrease much.

On the other hand, the peak mid-span displacement, peak ductility and the peak bearing displacement response decreases as the first period of the isolator increases. Peak base moment is not much influenced by the first period (T_1)

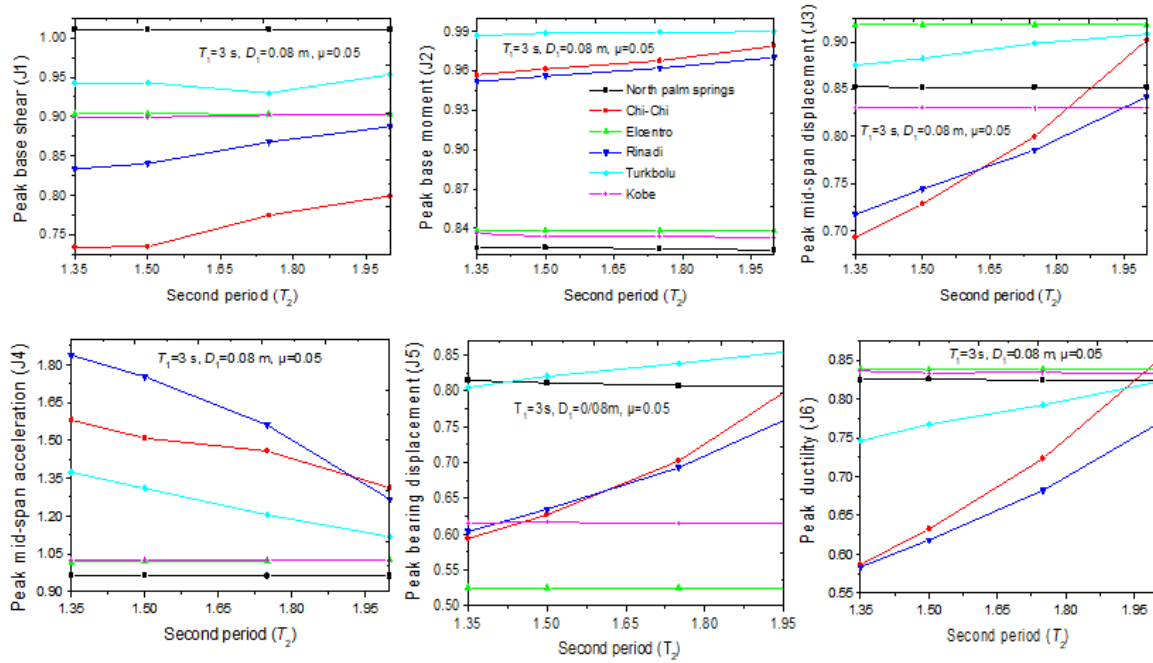


Fig. 6 Effect of Second period of PFPIs (T_2) on peak base shear, peak base moment, peak mid-span displacement, peak mid-span acceleration, peak bearing displacement and peak ductility

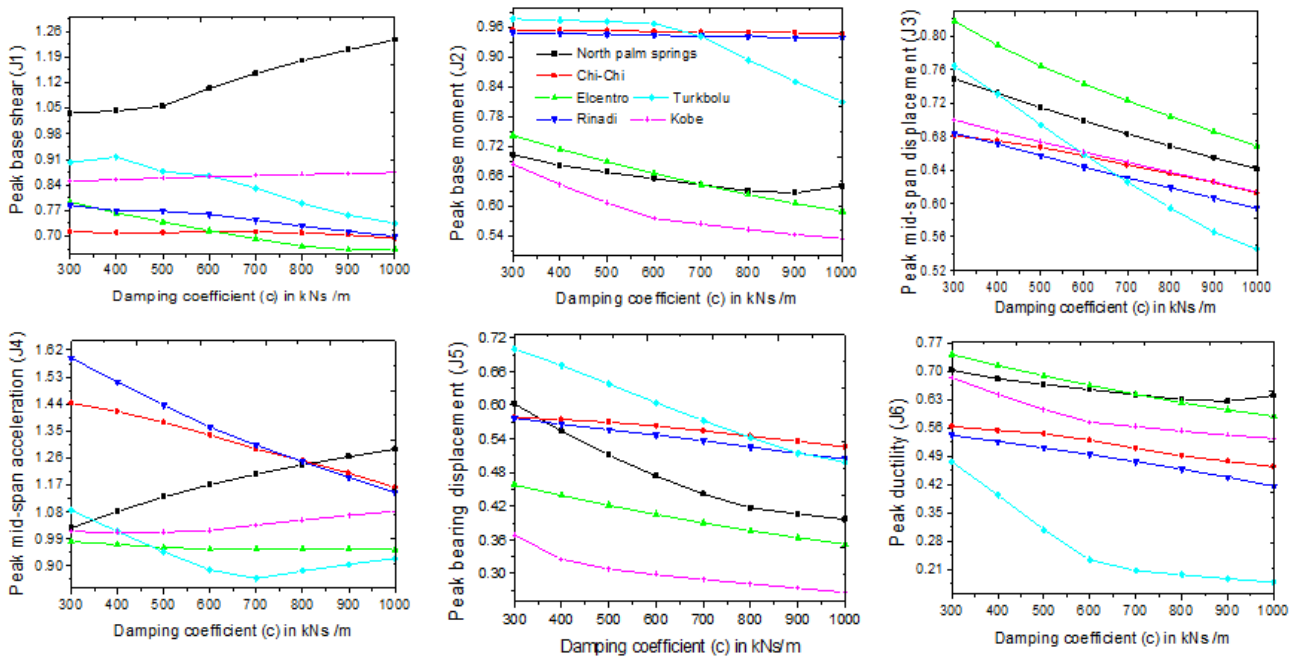


Fig. 7 Effect of the damping coefficient of VFD on peak base shear, peak base moment, peak mid-span displacement, peak mid-span acceleration, peak bearing displacement and peak ductility of the bridge with optimum parameters of the PFPI

of the PFPI. Due to an increase in the first period, the isolator remains in the lower stiffness region; therefore offering a better seismic response. The above variations conclude that an optimal first period is 3 sec. It is observed from Fig. 6, that peak responses such as base shear, mid-span displacement, bearing displacement and ductility increases with an increase in the second period (T_2). This is in agreement with the trend that the optimum first period (T_1) of the PFPI should be greater than the second period (T_2). Thus the optimal value can be considered as 1.35 sec.

From the parametric study performed, the optimum value of PFPI parameters considered are, first displacement (D_1)=0.08 m, first period (T_1)=3 s and second displacement (T_2)=1.35 s. The average coefficient of friction equivalent to 0.05 is considered for this study, which is a typical quality for a PTFE-stainless steel interface. Isolator is performing under two phases, one is a static phase or non sliding phase another one is a dynamic phase or sliding phase. In static phase, frictional force mobilized on the surface is less than the limiting frictional force; as a result isolator works as a

Table 3 Optimal parameters for hybrid control system

Parameters	Value	Parameters	Value
PFPI			
Initial period (T_0)	Infinite	First displacement (D_1)	0.08 m
First period (T_1)	3 sec	Second displacement (D_2)	0.12m
Second period (T_2)	1.35 sec	Coefficient of friction (μ)	0.05
PFPI + Linear VFD			
Damping coefficient (C)	900 kNs/m		
Velocity exponent (α)	1		
PFPI + Non-linear VFD			
Damping coefficient (C)	900 kNs/m		
Velocity exponent (α)	0.6		
PFPI + Non-linear FV spring damper			
Vibration period (T)	1.5 sec		
Damping coefficient (C)	1000 kNs/m		
Velocity exponent (α)	0.6		

conventionally fixed support. In dynamic phase frictional force exceeds the limiting frictional force, resulting the slider moved on the surface promoting high relative displacement between deck and the pier.

The behavior of the linear VFD can also be governed by damping coefficient (c) and velocity exponent (α) isolated from optimal parameters of the PFPI. Effect of damping coefficient on the variation of the evaluation criteria's (with an Optimal parameter of PFPI and velocity exponent=1) are plotted in Fig. 7. It can be observed from the Fig. 7 that,

with an increase in the damping coefficient of VFD peak mid-span and peak ductility response reduce significantly, with a massive decrease in the base displacement. This implies that there exists a particular value of the damping coefficient. It is observed from Fig. 7 that pier base shear reduces with an increase in the damping coefficient, which is giving an optimal value for all earthquakes except the North Palm Springs earthquake. For the North Palm Springs earthquake, the base shear is increasing rapidly when the damping coefficient exceeds 500 kNs/m for which no optimum value of the damping coefficient is found after it exceeds 500 kNs/m. After few iterations, the damping coefficient, $c=900$ kNs/m is considered for an optimal performance for all specified earthquakes except North Palm Springs earthquake.

Fig. 8 represents the result of the parametric study of the passive hybrid system consisting of PFPI with non-linear VFD. The variation of peak evaluation criteria of the isolated bridges against the velocity exponent (α) of VFD is shown in Fig. 8 for the six selected earthquakes in the benchmark highway bridge. A study has been performed varying the value of α from 0.4-2, keeping the value of the damping coefficient at the optimum level, (i.e., 900 kNs/m) and optimum PFPI parameters. It is observed from the Fig 8 that with an increase in α , Peak mid-span and bearing displacement increases. There exists a particular value of α , for which the peak base shear and base moment attains the minimum value. On the other hand, a peak mid-span acceleration first decreases rapidly attains the minimum value and then it is independent of the value of α . It is also revealed from Fig. 8 that optimum values lie between 0.4 and 0.6. Hence the optimum value of the velocity exponent is considered as 0.6, which holds optimum result for all earthquakes.

The result of the parametric study performed for the

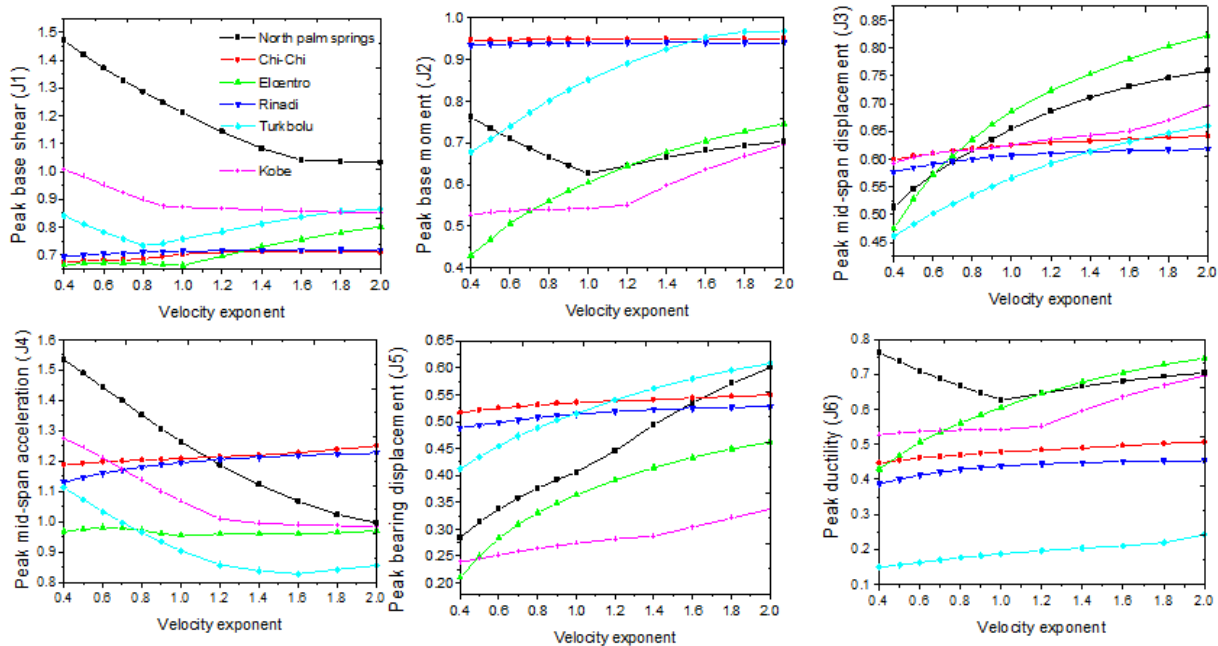


Fig. 8 Effect of velocity exponent of VFD on peak base shear, peak base moment, peak mid-span displacement, peak mid-span acceleration, peak bearing displacement and peak ductility of the bridge with optimum parameters of the PFPI

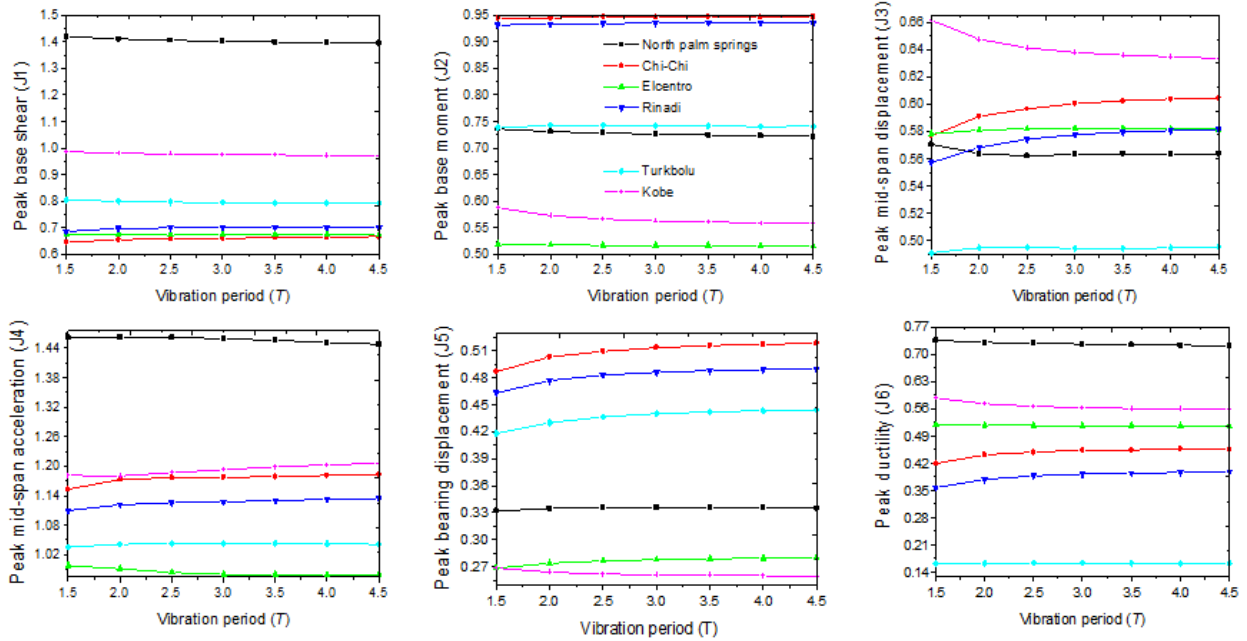


Fig. 9 Effect of vibration period of the FV spring damper on peak base shear, peak base moment, peak mid-span displacement, peak mid-span acceleration, peak bearing displacement and peak ductility of the bridge with optimum parameters of the PFPI

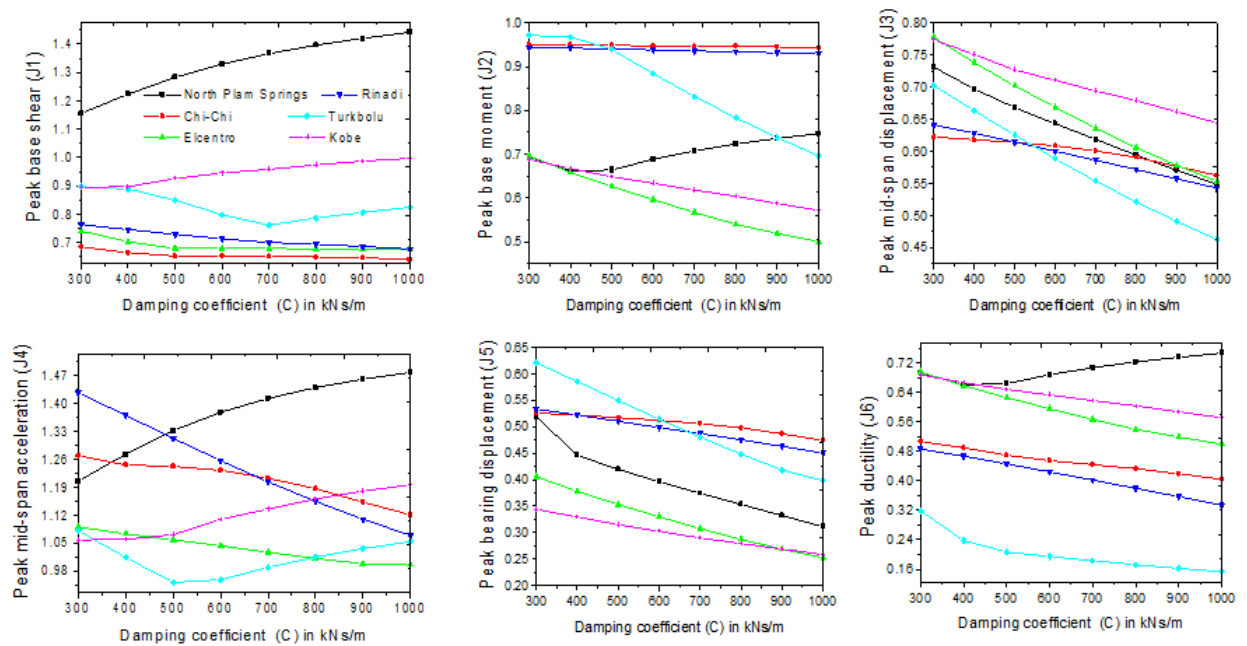


Fig. 10 Effect of the damping coefficient of the FV spring damper on peak base shear, peak base moment, peak mid-span displacement, peak mid-span acceleration, peak bearing displacement and peak ductility of the bridge with optimum parameters of the PFPI

passive hybrid system PFPI with non-linear FV spring damper is presented in Fig. 9. The variation of peak responses of the isolated benchmark bridge against the vibration period of the FV spring damper is shown in Fig. 9 for the six selected ground motions. From observations, it is revealed that peak base shear, base moment, mid-span acceleration are almost independent of vibration period. Although peak mid-span and bearing displacement responses are initially slightly influenced by the vibration

period. Hence $T=1.5$ sec is considered to be an optimal parameter for the non-linear FV spring damper for all earthquakes.

In order to investigate the effect of the damping coefficient of the non-linear FV spring damper, the variation of peak responses of the bridges with different damping coefficients obtained by the numerical analysis is plotted in Fig. 10. It is observed that increase in the damping coefficient of the FV spring damper reduces peak

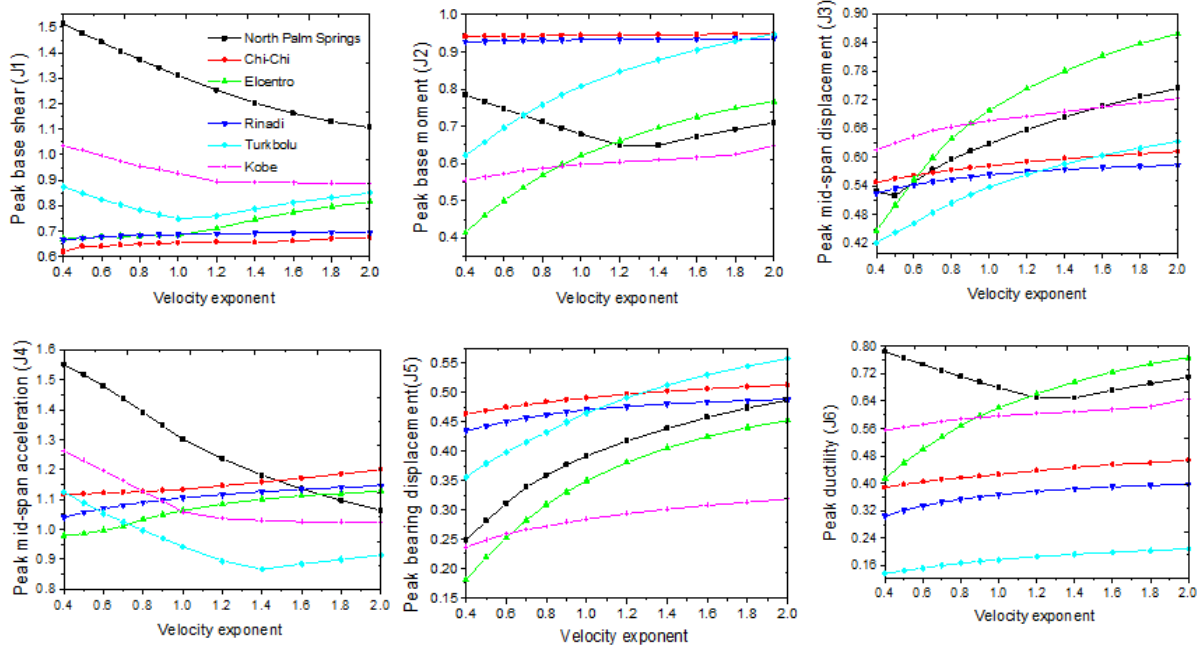


Fig. 11 Effect of velocity exponent of the FV spring damper on peak base shear, peak base moment, peak mid-span displacement, peak mid-span acceleration, peak bearing displacement and peak ductility of the bridge with optimum parameters of the PFPI

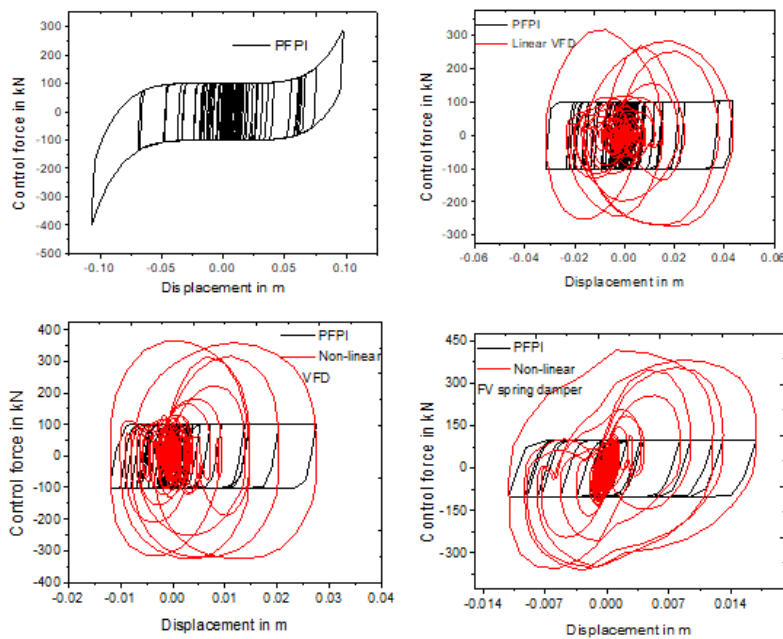


Fig. 12 Force-deformation behavior of the isolator with passive damper subjected to Ch-Chi earthquake

mid-span displacement and bearing displacement for all earthquakes. For both the North Palm Springs and Kobe earthquakes, pier base shear continues to increase with the increase in the damping coefficient of the non-linear FV spring damper, especially for North Palm Springs earthquake. There exists a particular value of the damping coefficient on which the peak base shear attains optimum for Turkbolu earthquake. The above observation implies that by designing an optimum FV spring damper, it is possible to reduce the mid-span displacement, bearing displacement and ductility response significantly, without

much increase in the peak base shear response. Thus the optimal value of the damping coefficient can be considered as 1000 kNs/m.

Fig. 11 represents the parametric study performed for the passive hybrid system. It can be observed that the peak base shear attains a minimum value for all earthquakes, except North Palm Springs earthquake, for which no optimum value of velocity exponent (α) is found up to 2 considered for the investigation. On the other hand with an increase in velocity exponent of FV spring damper, the peak mid-span displacement and bearing displacement increase

significantly. For the peak base moment response, it is observed in Fig. 11 that the optimal velocity exponent is found for the North Palm spring, Chi-Chi, Rinadi and Kobe earthquakes. For the Elcentro and Turkbolu earthquake, the peak base moment increases with an increase in velocity exponent. Peak mid-span acceleration response decreases with increase in the velocity exponent for North Palm Springs, Turkbolu and Kobe earthquakes.

5. Comparative study of the optimized value of the passive damper with PFPI.

The principal goal of the present study is to assess the performance of the passive dampers (linear or non-linear VFD and non-linear FV spring damper) with the PFPI system and compare its effectiveness with the PFPI alone system. Hence, the study is made to compare the passive hybrid system with optimized parameters.

In this endeavour, first the isolator/damper force and displacement (hysteresis loop) is studied for all of the hybrid systems for the optimized parameters, i.e., PFPI (T_0 =infinite, T_1 =3 sec, T_2 =1.35 sec, D_1 =0.08 m, D_2 =0.12 m and μ =0.05); linear VFD (c =900 kNs/m, α =1); non-linear VFD (c =900 kNs/m, α =0.6) and non-linear FV spring damper (T =1.5 sec, c =1000 kNs/m, α =0.6). Hysteresis loop of the different passive devices plays an important role in mitigation of the seismic response over a wide region. The force-displacement behaviour of the PFPI system alone and all other three-hybrid system are plotted under Chi-Chi earthquake ground motion. From hysteresis loop of the PFPI system alone, from Fig. 12 it has been observed that dual design performance can be achieved in terms of acceleration and displacement reduction. For earthquake ground motion, when the isolator displacement is below the first displacement (D_1 =0.08), PFPI reduces the acceleration response of the structure. On the other hand, when the isolator displacement exceeds the first displacement, PFPI protects the structure by reducing displacement response. The sharp change in restoring force is mainly due to the stiffness change of the PFPI system within the small relative displacement. For higher intensity ground motion such as Chi-Chi, the first displacement limit exceeded and the system was immediately pushed into a much higher stiffness region, which reduced the isolator efficiency; i.e., increased the mid-span acceleration. A very low value of initial horizontal stiffness is provided in order to achieve the first objective and, very high horizontal stiffness over small displacement is provided to achieve the second objective.

From earlier studies, the force-deformation characteristics of the viscous damper are adopted and reported in this study. The hysteresis loop of the linear VFD (α =1) is of a purely elliptical shape and for the non-linear VFD (α =0) it is rectangular in shape; the shape of the nonlinear damper with $0 < \alpha < 1$ falls between this elliptical and rectangular loop. It can be seen from this loop that non-linear VFD with velocity exponent less than one, dissipates more energy as compared to the linear VFD. For high-velocity shock, the peak control force of the non-linear VFD is limited or increases at a very low rate whereas the peak control force in linear VFD is increasing proportionately with the

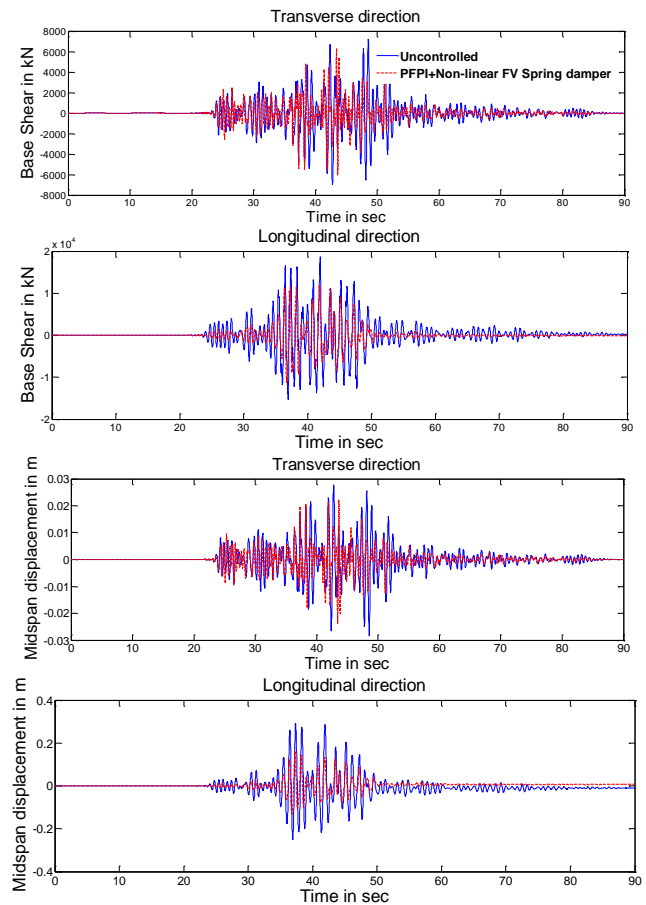


Fig. 13 Time history of base shear and mid-span displacement along the transverse and longitudinal direction under the Chi-Chi earthquake

velocity. Bearing displacement of the isolated bridge is the prime design parameter because at a higher bearing displacement the bearing of the bridge may fail, resulting in the collapse of the bridge. In reducing the bearing displacement of the bridge, all proposed hybrid systems work very well as compared to the PFPI alone systems, for a wide variety of earthquake ground motion records. Note that this response reduction is achieved without an increase in the pier base shear.

6. Evaluation criteria and comparison of the different control strategy

A set of numerical simulations of the highway bridges are performed in MATLAB for the six historical real earthquake ground motions namely, (i) North palm spring (1986) (ii) TUC084 component of Chi-Chi earthquake, Taiwan (1999) (iii) Elcentro component of Imperial Valley earthquake (iv) Rinadi component of Northridge (1984) (v) Bolu component of Duzce, Turkey (1999) earthquake (vi) Nishi-Akashi component of Kobe (1995) to verify the effectiveness and robustness of the proposed hybrid control strategy. Simulations of the test result are compared with that of the passive system. A more detailed description, including model description, considering ground motion

Table 4 Evaluation criteria of peak base shear, peak base moment, peak mid-span displacement and peak mid-span acceleration

Response quantity	Control strategy	North palm springs	Chi-Chi	Elcentro	Rinadi	Turkbolu	Kobe
Peak base shear (J_1)	PFPI	1.011	0.734	0.903	0.833	0.942	0.898
	PFPI + Linear VFD	1.209	0.703	0.663	0.713	0.757	0.871
	PFPI +Non-linear VFD	1.37	0.681	0.673	0.703	0.782	0.952
	PFPI +FV spring damper	1.441	0.639	0.676	0.676	0.824	0.996
Peak base moment (J_2)	PFPI	0.824	0.956	0.838	0.951	0.986	0.836
	PFPI + Linear VFD	0.626	0.949	0.604	0.939	0.851	0.542
	PFPI +Non-linear VFD	0.709	0.947	0.507	0.937	0.739	0.536
	PFPI +FV spring damper	0.747	0.942	0.5	0.929	0.696	0.571
Peak mid-span displacement (J_3)	PFPI	0.852	0.692	0.918	0.717	0.875	0.83
	PFPI + Linear VFD	0.654	0.624	0.685	0.606	0.565	0.625
	PFPI +Non-linear VFD	0.572	0.61	0.572	0.59	0.502	0.61
	PFPI +FV spring damper	0.548	0.562	0.553	0.542	0.462	0.644
Peak mid-span acceleration (J_4)	PFPI	0.962	1.58	1.016	1.837	1.373	1.026
	PFPI + Linear VFD	1.264	1.208	0.955	1.194	0.904	1.068
	PFPI +Non-linear VFD	1.443	1.197	0.981	1.16	1.034	1.21
	PFPI +FV spring damper	1.478	1.121	0.995	1.069	1.053	1.196
Peak bearing displacement (J_5)	PFPI	0.814	0.593	0.525	0.603	0.804	0.615
	PFPI + Linear VFD	0.406	0.535	0.363	0.513	0.514	0.273
	PFPI +Non-linear VFD	0.337	0.524	0.283	0.498	0.455	0.252
	PFPI +FV spring damper	0.31	0.474	0.252	0.45	0.398	0.258
Peak ductility (J_6)	PFPI	0.824	0.586	0.838	0.583	0.746	0.836
	PFPI + Linear VFD	0.626	0.477	0.604	0.438	0.187	0.542
	PFPI +Non-linear VFD	0.709	0.461	0.507	0.411	0.162	0.536
	PFPI +FV spring damper	0.747	0.404	0.5	0.334	0.153	0.571

and evaluation criteria of the benchmark highway bridge, can be found to be a definitional problem in the paper Agrawal *et al.* (2005, 2009). In the sample control problem of the benchmark highway bridge, the sixteen devices are implemented (a total number of eight locations at each end) at the two abutments. The distribution of control strategy is identical to the sample control system of the bridge in order to facilitate a valid comparison among them. The result of peak and norm value of different response quantities for PFPI with linear or non-linear VFD and non-linear FV spring damper, such as peak and norm base shear (J_1 and J_9), peak and norm base moment (J_2 and J_{10}), peak and norm mid-span displacement (J_3 and J_{11}), peak and norm mid-span acceleration (J_4 and J_{12}), peak and norm bearing displacement (J_5 and J_{13}), peak and norm ductility (J_6 and J_{13}) are presented in Tables 4 and 5, respectively. It is observed from evaluation criteria that for strong earthquakes, such as Chi-Chi and Rinadi, the result obtained with a passive hybrid system (PFPI with FV spring damper) yields the best result in reducing base shear response as compared to the PFPI isolation system alone and other hybrid systems. The response reduction is observed to be 37% and 33%, respectively, for the Chi-Chi and Rinadi earthquakes.

For North Palm Springs earthquake passive hybrid system has failed to control the base shear response. For medium intensity earthquakes such as Elcentro, Turkbolu, and Kobe, the performance of PFPI with linear VFD is

comparable to the other control strategies in reducing base shear response. On an average, base shear response is best controlled by the passive hybrid system as compared to the PFPI alone system. It is observed from evaluation of Table 4, that in reducing base moment all passive hybrid systems have better performance than PFPI alone system. During Elcentro earthquake while PFPI acting with FV spring damper or non-linear VFD, the maximum reduction in the base moment was around 50% as compared to 33% more reduction with PFPI alone. The maximum base moment reduction by PFPI with linear VFD and PFPI alone are around 46% and 17% during the Kobe earthquake. In reducing mid-span displacement passive hybrid system is more significant than PFPI alone system for all six earthquakes. The peak mid-span displacement is reduced to within a range of 36% to 54% for PFPI with FV spring damper. This result is comparable to the PFPI alone system too. For Chi-Chi, Elcentro, Rinadi and Turkbolu earthquakes PFPI with FV spring damper are more promising in reducing mid-span acceleration. This control strategy improves mid-span acceleration response which is more comparable to the other control systems. As observed from Table 5, the bearing displacement is substantially reduced by the passive hybrid system compared to the PFPI alone. The PFPI with FV spring damper can reduce 75% bearing displacement during Elcentro and Kobe earthquakes. For North Palm Spring earthquake the bearing displacement reduction (PFPI with F_v spring damper) is

Table 5 Evaluation criteria of peak base shear, peak base moment, peak mid-span displacement and peak mid-span acceleration

Response quantity	Control strategy	North palm springs	Chi-Chi	Elcentro	Rinadi	Turkbolu	Kobe
Norm base shear (J_9)	PFPI	0.84	0.861	0.646	0.808	0.878	0.763
	PFPI + Linear VFD	1.027	0.722	0.555	0.672	0.749	0.758
	PFPI +Non-linear VFD	1.138	0.662	0.562	0.633	0.788	0.811
	PFPI +FV spring damper	1.183	0.611	0.571	0.598	0.814	0.844
Norm base moment (J_{10})	PFPI	0.766	0.829	0.613	0.832	0.812	0.728
	PFPI + Linear VFD	0.544	0.722	0.41	0.697	0.354	0.53
	PFPI +Non-linear VFD	0.562	0.687	0.29	0.67	0.301	0.445
	PFPI +FV spring damper	0.584	0.583	0.288	0.686	0.273	0.448
Norm mid-span displacement (J_{11})	PFPI	0.786	0.741	0.631	0.697	0.746	0.752
	PFPI + Linear VFD	0.573	0.586	0.427	0.578	0.425	0.559
	PFPI +Non-linear VFD	0.473	0.546	0.304	0.549	0.364	0.471
	PFPI +FV spring damper	0.466	0.46	0.274	0.484	0.329	0.473
Norm mid-span acceleration (J_{12})	PFPI	0.96	1.051	0.777	1.058	1.021	0.89
	PFPI + Linear VFD	1.002	0.81	0.777	0.832	1.012	1.06
	PFPI +Non-linear VFD	1.11	0.755	0.812	0.806	1.079	1.161
	PFPI +FV spring damper	1.138	0.753	0.831	0.811	1.103	1.202
Norm bearing displacement (J_{13})	PFPI	0.484	0.689	0.406	0.647	0.568	0.411
	PFPI + Linear VFD	0.255	0.543	0.256	0.524	0.276	0.2
	PFPI +Non-linear VFD	0.196	0.507	0.166	0.495	0.233	0.16
	PFPI +FV spring damper	0.177	0.402	0.131	0.415	0.2	0.15
Norm ductility (J_{14})	PFPI	0.766	0.482	0.613	0.561	0.818	0.728
	PFPI + Linear VFD	0.544	0.506	0.41	0.873	0.034	0.53
	PFPI +Non-linear VFD	0.562	0.613	0.29	0.772	0.029	0.445
	PFPI +FV spring damper	0.584	0.44	0.288	0.804	0.026	0.448

69%, compared to a 50% more reduction by PFPI alone system and for Turkbolu earthquake corresponding values are 61% and 41% respectively. For higher intensity earthquake, the response is significantly reduced by PFPI with FV spring damper system compared to all the other control systems, especially PFPI alone system. The present investigation indicates that Passive hybrid system is more significant than PFPI alone system in reducing ductility response. For strong earthquakes such as Chi-Chi and Rinadi earthquakes, PFPI with FV spring-damper system is more efficient in controlling ductility response of the bridges. The result of the simulation indicates that passive hybrid system, especially PFPI with FV spring damper is more effective in reducing base shear, base moment, mid-span acceleration, mid-span displacement and bearing displacement, and ductility response. Bearing displacement response is the main design aspect of the isolated bridge, the main reason behind this is that if bearing displacement exceeds a certain limit; the bearing may come up resulting into the collapse of the bridge.

This evaluation criteria indicates that passive hybrid control system can reduce the peak bearing displacement of the bridge without sacrificing the benefits of the base isolated system in the reduction of peak base shear and the peak mid-span acceleration compared to the isolation alone system. The relative better performance of the PFPI and Non-linear FV spring damper hybrid system as compared to the isolation system alone is not due to the hysteretic

damping or the energy dissipation through friction as there are not many force reversal cycles. The better performance can be attributed due to the stiffening effect of the isolator under pulse type near fault ground motions. The stiffening effect resulting in an effective period of the isolated structure has shifted from the typical pulse period of the near fault ground motions. Thus the period of the Non-linear FV spring damper (Which is contributed to the stiffening effect of the inclined hysteresis behavior) is selected such a way that will provide enough rigidity and shifting the isolation period away from the typical pulse type period associated with the near fault ground motions. This will provide enough potential benefits of the base isolated system for reducing the seismic responses.

Figure 13 demonstrate the time variation of the base shear and mid-span displacement in transverse and longitudinal direction, respectively for Chi-Chi earthquake. The result shows that there is an extensive reduction in base shear and mid-span displacement with PFPI and non-linear FV spring damper compared to the uncontrolled response.

The numerical simulation indicates that proposed passive hybrid system is much better in terms of mitigating response compared to that PFPI isolation system alone. The result of the investigation demonstrated that passive hybrid control system is capable of reducing displacement response of the benchmark highway bridge with little increase or no increase in pier base shear and mid-span acceleration response as a resulting reducing the length of

expansion joints of the bridge. Based on the evaluation criteria it is concluded that the proposed hybrid control system might be the right choice for the benchmark highway bridge in reducing seismic response. Hence the use of the VFD and FV spring damper as a supplement device with PFPI system is effective to solve the super structural displacement response of the benchmark highway bridge, along with controlling the other response such as base shear, base moment, acceleration and ductility for a wide variety of earthquake records. Numerical simulation performed for all six earthquake ground motions indicates that the PFPI system with non-linear FV spring damper is more promising to reduce seismic response that is compared to the other hybrid system.

7. Conclusions

The behavior of the passive hybrid system in controlling the seismic response of the benchmark highway bridge subjected to two directional (ignoring vertical ground motion component) six earthquakes ground motion is investigated in order to study different parameters of the control strategy. The hybrid control system consists of PFPI with linear and non-linear VFD and non-linear FV spring damper. The seismic response of a simplified numerical model of the 91/5 highway overcrossing is located in Southern California. The seismic response of the benchmark highway bridge with PFPI system alone and with the hybrid system has been investigated. The responses of the isolated benchmark bridge are plotted under different parameters of the PFPI, linear and non-linear VFD and Non-linear FV spring damper. At last, an optimum response for all criteria is provided in terms of base shear, base moment, mid-span and bearing displacement, mid-span acceleration, and ductility. Seismic response of the benchmark bridge with the passive hybrid system is compared with that of the bridge with PFPI system alone. From the analytical seismic response investigation of the benchmark bridge with the passive hybrid control system, the following conclusions can be drawn:

- i) The numerical simulation result indicates that passive hybrid system helps to reduce the seismic response of the benchmark bridge in comparison to the PFPI system alone, such as base shear, base moment, acceleration response, ductility response. Although PFPI with non-linear FV spring damper is more effective in reducing the displacement response of the bridge for all earthquakes, especially for strong earthquakes Chi-Chi and Rinadi earthquakes.
- ii) The inclined hysteresis loop (Due to the spring stiffness) of the non-linear FV spring damper with softening behaviour of the PFPI system is more effective in reducing the seismic response. Specifically, non-linear FV spring dampers with vibration period of the spring and velocity exponent are equal to 1.5 sec and 0.6, which is found to be very effective in reducing displacement response.
- iii) PFPI with Non-linear FV spring damper hybrid system is quite effective in reducing the seismic

response of the bridge without much increase in the acceleration response under the pulse type near-fault ground motions.

iv) With the passive hybrid system, the maximum reduction response in the bearing displacement can be achieved, up to about 75%.

vi) Based on the result, it is concluded that the proposed hybrid control strategy may be the right choice for the benchmark highway bridge compared to the PFPI system alone.

vi) Passive hybrid control system consists of base isolation bearing and passive dampers which is often reliable, very easy installation and very cost-effective approaches in the mitigation of the effects of strong ground motion. However, the effectiveness of the all passive hybrid systems depends on the time history response of the earthquake ground motion.

References

- Abdel Raheem, S.E. and Hayashikawa, T. (2013), "Energy dissipation system for earthquake protection of cable-stayed bridge towers", *Earthq. Struct.*, **5**(6), 657-678.
- Agrawal, A., Tan, P., Nagarajaiah, S. and Zhang, J. (2009), "Benchmark structural control problem for a seismically excited highway bridge-Part I: Phase I problem definition", *Struct. Control Health Monit.*, **16**, 509-529.
- Agrawal, A.K. *et al.* (2005), "Benchmark structural control problem for a seismically excited bridge, Part I; Problem definition", <http://www-ce.emgr.cuny.cuny.edu/people/Agrawal>.
- Amiri, G.G., Shakouri, A., Veismoradi, S. and Namiranian, P. (2017), "Effect of seismic pounding on building isolated by triple friction pendulum bearing", *Earthq. Struct.*, **12**(1), 35-45.
- Chen, B., Sun, Y.Z., Li, Y.L. and Zhao, S.L. (2014), "Control of seismic response of a building frame by using hybrid system with Magneto rheological dampers and isolators", *Adv. Struct. Eng.*, **17**(8), 1199-1215.
- Dicleli, M. (2007), "Supplemental elastic stiffness to reduce isolator displacements for seismic-isolated bridges in near-fault zones", *Eng. Struct.*, **29**, 763-775.
- Geng, F., Ding, Y., Song, J., Li, W. and Li, A. (2014), "Passive control system for seismic protection of a multi-tower cable-stayed bridge", *Earthq. Struct.*, **6**(5), 495-514.
- Hall, J.F., Heaton, T.H., Halling, M.W. and Wald, D.J. (1995), "Near-source ground motion and its effects on flexible buildings", *Earthq. Spectra*, **11**, 569-605.
- He, W.L. and Agrawal, A.K. (2007), "Passive and hybrid control systems for seismic protection of benchmark cable-stayed bridge", *Struct. Control Health Monit.*, **14**, 1-26.
- Heaton, T.H., Hall, J.F., Wald, D.J. and Halling, M.W. (1995), "Response of high-rise and base-isolated buildings to a hypothetical MW7.0 blind thrust earthquake", *Sci.*, **267**, 206-211.
- Jangid, R.S. (2004), "Seismic response of isolated bridges", *J. Bridge Eng.*, **9**(2), 156-166.
- Kataria, N.P. and Jangid, R.S. (2016), "Seismic protection of the horizontally curved bridge with semi-active variable stiffness damper and isolation system", *Adv. Struct. Eng.*, **19**(7), 1103-1117.
- Lu, L.Y., Lee, T.Y., Juang, S.Y. and Yeh, S.W. (2013), "Polynomial Friction Pendulum Isolators (PFPIs) for building floor isolation: An experimental and theoretical study", *Eng. Struct.*, **56**, 970-982.

- Markou, A.A., Oliveto, G. and Athanasiou, A. (2016), "Response simulation of hybrid simulation systems under earthquake excitation", *Soil Dyn. Earthq. Eng.*, **84**, 120-133.
- Matsagar, V.A. and Jangid, R.S. (2008), "Base isolation for seismic retrofitting of structures", *Pract. Period. Struct. Des. Constr.*, **13**(4), 175-185.
- Mishra, S.K., Gur, S., Roy, K. and Chakraborty, S. (2015), "Response of bridges isolated by shape memory-alloy rubber bearing", *J. Bridge Eng.*, **21**(2), 04015071.
- Nakata, S., Hanai, T., Kiriyama, S.I. and Fukuwa, N. (2004), "Comparison of seismic performance of base-isolated house with various devices", *J. Struct. Eng. B*, **50B**, 561-574.
- Park, K.S., Jung, H.J., Spencer, B.F. and Lee, I.W. (2003), "Hybrid control systems for seismic protection of a phase II benchmark cable-stayed bridge", *J. Struct. Control*, **10**, 231-247.
- Saha, A., Saha, P. and Patro, S.K. (2015), "Seismic response control of benchmark highway bridge using non-linear FV spring damper", *IES J. Past A: Civil Struct. Eng.*, **8**(4), 240-250.
- Shakib, H. and Fuladgar, A. (2003), "Response to pure-friction sliding structures to three component earthquake excitation", *Comput. Struct.*, **81**, 189-196.
- Soneji, B.B. and Jangid, R.S. (2007), "Passive hybrid system for seismic protection of cable-stayed bridge", *Eng. Struct.*, **29**, 57-70.
- Sorace, S. and Terenzi, G. (2001), "Non-linear dynamic modeling and design procedure of FV spring dampers for base isolation", *Eng. Struct.*, **23**, 1556-1567.
- Sorace, S. and Terenzi, G. (2001), "Non-linear dynamic modeling and design procedure of FV spring- dampers for base isolation-frame building applications", *Eng. Struct.*, **23**, 1568-1576.
- Takewaki, I., Kanamori, M., Yoshitomi, S. and Tsuji, M. (2013), "New experimental system for base isolated structures with various dampers and limit aspect ratio", *Earthq. Struct.*, **5**(4), 461-475.
- Wen, Y.K. (1976), "Method for random vibration of hysteretic systems", *J. Eng. Mech.*, ASCE, **102**, 249-263.
- Xie, W. and Sun, L. (2014), "Passive hybrid system for seismic failure mode improvement of a long-span cable-stayed bridges in transverse direction", *Adv. Struct. Eng.*, **17**(8), 399-411.
- Xing, S., Camara, A. and Aijun, Y. (2015), "Effects of seismic devices on transverse responses of piers in the Sutong Bridge", *Earthq. Eng. Eng. Vib.*, **14**(4), 611-623.